The Company of Biologists

RESEARCH ARTICLE

Optogenetic activation reveals distinct roles of PIP_3 and Akt in adipocyte insulin action

Yingke Xu[1,2,*], Di Nan[1], Jiannan Fan[1], Jonathan S. Bogan[2,3] and Derek Toomre[2,*]

ABSTRACT

Glucose transporter 4 (GLUT4; also known as SLC2A4) resides on intracellular vesicles in muscle and adipose cells, and translocates to the plasma membrane in response to insulin. The phosphoinositide 3-kinase (PI3K)–Akt signaling pathway plays a major role in GLUT4 translocation; however, a challenge has been to unravel the potentially distinct contributions of PI3K and Akt (of which there are three isoforms, Akt1–Akt3) to overall insulin action. Here, we describe new optogenetic tools based on CRY2 and the N-terminus of CIB1 (CIBN). We used these 'Opto' modules to activate PI3K and Akt selectively in time and space in 3T3-L1 adipocytes. We validated these tools using biochemical assays and performed live-cell kinetic analyses of IRAP–pHluorin translocation (IRAP is also known as LNPEP and acts as a surrogate marker for GLUT4 here). Strikingly, Opto-PIP_3 largely mimicked the maximal effects of insulin stimulation, whereas Opto-Akt only partially triggered translocation. Conversely, drug-mediated inhibition of Akt only partially dampened the translocation response of Opto-PIP_3. In spatial optogenetic studies, focal targeting of Akt to a region of the cell marked the sites where IRAP–pHluorin vesicles fused, supporting the idea that local Akt-mediated signaling regulates exocytosis. Taken together, these results indicate that PI3K and Akt play distinct roles, and that PI3K stimulates Akt-independent pathways that are important for GLUT4 translocation.

KEY WORDS: Optogenetics, Insulin signaling, TIRFM, Glucose transporter, Exocytosis

INTRODUCTION

Insulin is a potent anabolic hormone, which plays key roles in energy metabolism, growth and cellular differentiation. A major physiological action of insulin is to increase glucose uptake in muscle and fat cells. Insulin stimulates glucose uptake by mobilizing intracellular vesicles containing GLUT4 (also known as SLC2A4) glucose transporters. These GLUT4 storage vesicles (GSVs) fuse with the plasma membrane (Bogan, 2012; Leto and Saltiel, 2012; Stockli et al., 2011). Insulin-regulated GLUT4 translocation is crucial for maintaining glucose homeostasis in mammals, and impaired translocation results in insulin resistance

and contributes to type 2 diabetes in humans (Kahn and Flier, 2000; Stolar, 2002).

Insulin action is initiated through binding and activation of its surface receptor. Diverse functions are then achieved by signal propagation through a network of interconnecting proteins and cascades (Saltiel and Pessin, 2002; Taniguchi et al., 2006). In the canonical insulin-signaling pathway, activation of the insulin receptor leads to the phosphorylation of insulin receptor substrates and activation of phosphoinositide 3-kinase (PI3K). It is well established that activation of PI3K is necessary for insulin-stimulated GLUT4 translocation, as several studies have shown that the inhibition of PI3K activity blocks insulin-stimulated GLUT4 translocation, whereas manipulations that increase phosphatidylinositol (3,4,5)-trisphosphate (PIP_3) levels in the absence of insulin induce GLUT4 translocation and glucose uptake (Martin et al., 1996; Sweeney et al., 2004; Tanti et al., 1996). Activated PI3K increases the conversion of phosphatidylinositol 4,5-bisphosphate [PIP_2] to PIP_3 at the plasma membrane. In turn, this recruits Akt (of which there are three isoforms, Akt1–Akt3) to phosphoinositide-dependent kinase-1 (PDK1) and the mechanistic target of rapamycin complex-2 (mTORC2) so that Akt is phosphorylated by these enzymes at residues Thr308 and Ser473, respectively, and is thus activated. Knockdown and knockout studies have shown that Akt, particularly the Akt2 isoform, is required for insulin-stimulated GLUT4 translocation (Cho et al., 2001a,b; Jiang et al., 2003; Katome et al., 2003; McCurdy and Cartee, 2005). Studies in which constitutively active Akt2 has been overexpressed, or in which chemical-genetic approaches have been used to activate Akt2 acutely, suggest that Akt2 alone is fully sufficient to stimulate GLUT4 translocation (Kohn et al., 1996; Ng et al., 2010b, 2008). However, comparison of GLUT4 translocation after acute Akt2 activation has been made only upon submaximal insulin stimulation, and it remains unclear how the data fit with the less-well-studied non-PI3K and non-Akt signals that are required for insulin-stimulated GLUT4 translocation (Bogan et al., 2012; Chang et al., 2007; Chiang et al., 2001; Farese et al., 2007; Klip et al., 2014; Sajan et al., 2014b; Sylow et al., 2014; Ueda et al., 2010; Cheney et al., 2011; Govers et al., 2004; Martinez et al., 2010). In particular, although PI3K and Akt are two major signaling nodes in insulin-regulated GLUT4 trafficking, previous studies have not examined the individual contributions of acute activation of each of these kinases separately and have not compared the overall effect with that of maximal insulin stimulation.

The complexity of the insulin signaling network and interplay between different signaling components make it challenging to resolve the distinct roles of specific signaling molecules. Standard manipulations (knockdown, overexpression and mutation) have chronic effects and can cause secondary phenomena or cell compensation. Pharmacological perturbations can rapidly turn on or off the function of a target protein, but they provide no spatial information and commonly cause off-target effects. Optogenetics permits manipulation of intracellular signaling pathways using light-mediated protein heterodimerization and homodimerization

[1]Department of Biomedical Engineering, MOE Key Laboratory of Biomedical Engineering, Zhejiang Provincial Key Laboratory of Cardio-Cerebral Vascular Detection Technology and Medicinal Effectiveness Appraisal, Zhejiang University, Hangzhou 310027, China. [2]Department of Cell Biology, Yale University School of Medicine, New Haven, 06510, USA. [3]Section of Endocrinology and Metabolism, Department of Internal Medicine, Yale University School of Medicine, New Haven, CT 06520-8020, USA.

*Authors for correspondence (yingkexu@zju.edu.cn; derek.toomre@yale.edu)

Y.X., 0000-0002-8317-0608; J.F., 0000-0002-6392-8493; J.S.B., 0000-0001-6463-8466; D.T., 0000-0002-6827-8127

(Gautier et al., 2014; Pathak et al., 2013). Optogenetic approaches provide a potential solution to the problem of dissecting cellular network function (Toettcher et al., 2011). To date, various optogenetic modules have been introduced to manipulate intracellular protein activities (Xu et al., 2011a). One is based on a basic helix-loop-helix protein *Arabidopsis* CIB1 (also known as BHLH63) and cryptochrome 2 (CRY2) (Kennedy et al., 2010). Blue-light illumination induces the heterodimerization of CRY2 with the N-terminus of CIB1 (CIBN). This reaction is rapid, with response times in the order of sub-seconds, and does not require exogenous cofactors (Idevall-Hagren et al., 2012; Kennedy et al., 2010).

In the present study, we applied two optogenetic tools based on the CRY2–CIBN optogenetic system, which we name 'Opto-PIP_3' and 'Opto-Akt', respectively. These optogenetic modules enable us to 'walk down' the insulin-signaling cascade by selectively activating PI3K and Akt activities with light. We can thus probe the differential effects of insulin and of these molecules to stimulate GLUT4 exocytosis in 3T3-L1 adipocytes. We found that except for an initial delay, light-induced PIP_3 mimicked the effect of insulin and strongly stimulated the plasma membrane translocation of the GSV cargo, IRAP (also known as LNPEP). In comparison, optogenetically activated Akt2 only partially stimulated translocation. Our study revealed that insulin signals act not only globally but also locally because site-specific activation of Akt precisely marked where the vesicles fuse. Finally, the tools we developed will have broad application in other systems to analyze the transmission properties of growth factors, PI3K and Akt, and to elucidate their dynamics and distinct effects.

RESULTS
Optogenetic control of PIP_3 production in 3T3-L1 adipocytes
The optogenetic system we used is based on *Arabidopsis thaliana* cryptochrome 2 (CRY2) and the transcription factor CIBN; this system requires no cofactors, works with standard wavelengths and light-induced heterodimerization of the two proteins is relatively fast (Kennedy et al., 2010). Our first target was PIP_3, a crucial signaling node in insulin signaling. Based on our previous work, we used a CRY2–iSH2 fusion protein (Idevall-Hagren et al., 2012). This protein binds to endogenous PI3K p110α catalytic subunits constitutively. We predicted that, upon blue-light activation, CRY2–iSH2 would be recruited to the plasma membrane of 3T3-L1 adipocytes expressing a CaaX-tagged CIBN binding partner. In turn, this should allow the plasma-membrane-recruited PI3K to generate PIP_3 in an acute manner, which we monitored using a PIP_3 reporter, PH-Akt-mRFP (where 'PH-Akt' indicates the plextrin homology domain of Akt Fig. 1A). We term this optogenetic system 'Opto-PIP_3'. As anticipated, in 3T3-L1 adipocytes that had been co-transfected with mCherry–CRY2–iSH2 and CIBN–pmGFP (CIBN tagged with a CaaX motif and GFP), blue light triggered the rapid recruitment of mCherry–CRY2–iSH2 from the cytosol to the plasma membrane, with a response half time ($t_{1/2}$) of 2.4±0.5 s (mean±s.e.m.; Fig. 1B and C; Movie 1).

To monitor PIP_3 generation at the plasma membrane, we used a PH-Akt–mRFP reporter together with total internal reflection fluorescence microscopy (TIRFM). We substituted unlabeled CRY2–iSH2 for mCherry–CRY2–iSH2 so that we could visualize plasma membrane recruitment of the fluorescent PIP_3 sensor (Tengholm and Meyer, 2002). As shown in Fig. 1D and E, upon blue-light stimulation, the intensity of PH-Akt–mRFP near to the cell surface rapidly increased ∼1.8 fold, and when the blue light was turned off, the signal slowly dropped back to baseline

($t_{1/2off}$=345±15 s). To demonstrate the reversibility of the reaction, three sequential light–dark cycles were performed, each of which reversibly stimulated PIP_3 generation (see Movie 2). The Opto-PIP_3-induced PIP_3 production depended on PI3K enzymatic activity because the addition of the established PI3K inhibitor wortmannin caused PH-Akt–mRFP on the membrane to rapidly diminish (Fig. 1E). The potency of Opto-PIP_3 and insulin-induced surface PIP_3 production were quantitatively analyzed and, as shown in Fig. 1F, the maximum recruitment of PH-Akt–mRFP to the plasma membrane was nearly identical using Opto-PIP_3 compared to that upon treatment with 100 nM insulin. Strikingly, the kinetics of PIP_3 generation were different, and stimulation using 100 nM insulin ($t_{1/2}$=59±7 s) was faster than stimulation using Opto-PIP_3 ($t_{1/2}$=98±8 s).

Opto-PIP_3 causes Akt phosphorylation in an insulin-independent manner
We next sought to test whether Opto-PIP_3 (Idevall-Hagren et al., 2012) could specifically activate downstream Akt signaling and bypass other insulin-dependent signaling pathways. 3T3-L1 adipocytes were transiently electroporated with CRY2–iSH2 and CIBN–CaaX, and a light-emitting diode (LED) box was used to trigger optogenetic heterodimerization. The status of signaling activation was tested by western blotting. As shown in Fig. 2A, Opto-PIP_3 caused the phosphorylation of endogenous Akt (the antibody used recognizes all Akt isoforms) on both residues Thr308 and Ser473 (Fig. 2A). The lower levels of phosphorylation in response to Opto-PIP_3, compared with those in response to insulin stimulation, are likely to be because only ∼20% of the adipocytes were transfected in this experiment (see below). As an important control, ERK1/2 (also known as MAPK3 and MAPK1), which is a downstream target of activated insulin receptor (Taniguchi et al., 2006), was phosphorylated only by insulin and not in response to blue LED light (Fig. 2A).

Next, we used immunofluorescence staining of phosphorylated (phospho)-Akt to quantitatively analyze Akt phosphorylation in individual cells. 3T3-L1 adipocytes were transiently electroporated with CRY2–iSH2 and CIBN–pmGFP. The cells were kept in the dark or optically triggered with an LED box to induce PI3K activation. For comparison, control adipocytes were treated with 10 nM or 100 nM insulin. The transfected adipocytes were identified by GFP signals under a spinning disk confocal microscope (Fig. 2B; Fig. S1). Maximum z-projection images were generated, and the phospho-Akt fluorescence signals were quantified. As expected, insulin stimulated Akt phosphorylation at both Thr308 and Ser473, and did so in a concentration-dependent manner (Fig. S1A and B). The staining of phospho-Akt, both at Thr308 and Ser473, was similar in cells that had been stimulated using blue light (Fig. 2C; Fig. S1D). Because the electroporated cells express variable amounts of the constructs, the transfected cells displayed different levels of responsiveness to light (Fig. 2B). Strikingly, in the highly responsive transfected cells (marked 'H' in Fig. 2 and Fig. S1), Opto-PIP_3 activation generated phospho-Akt signals that were comparable to those stimulated by 100 nM insulin (Fig. 2C; Fig. S1D). Importantly, both insulin- and light-induced Akt phosphorylation were abolished in cells that had been pre-treated with wortmannin or Akt inhibitor (Fig. 2B; Fig. S1E).

Opto-PIP_3 promotes GLUT4 vesicle exocytosis in 3T3-L1 adipocytes
The above studies suggest that Opto-PIP_3 not only recruits Akt but also causes its phosphorylation at Thr308 and Ser473. Hence, we tested whether Opto-PIP_3 promotes GLUT4 exocytosis. 3T3-L1
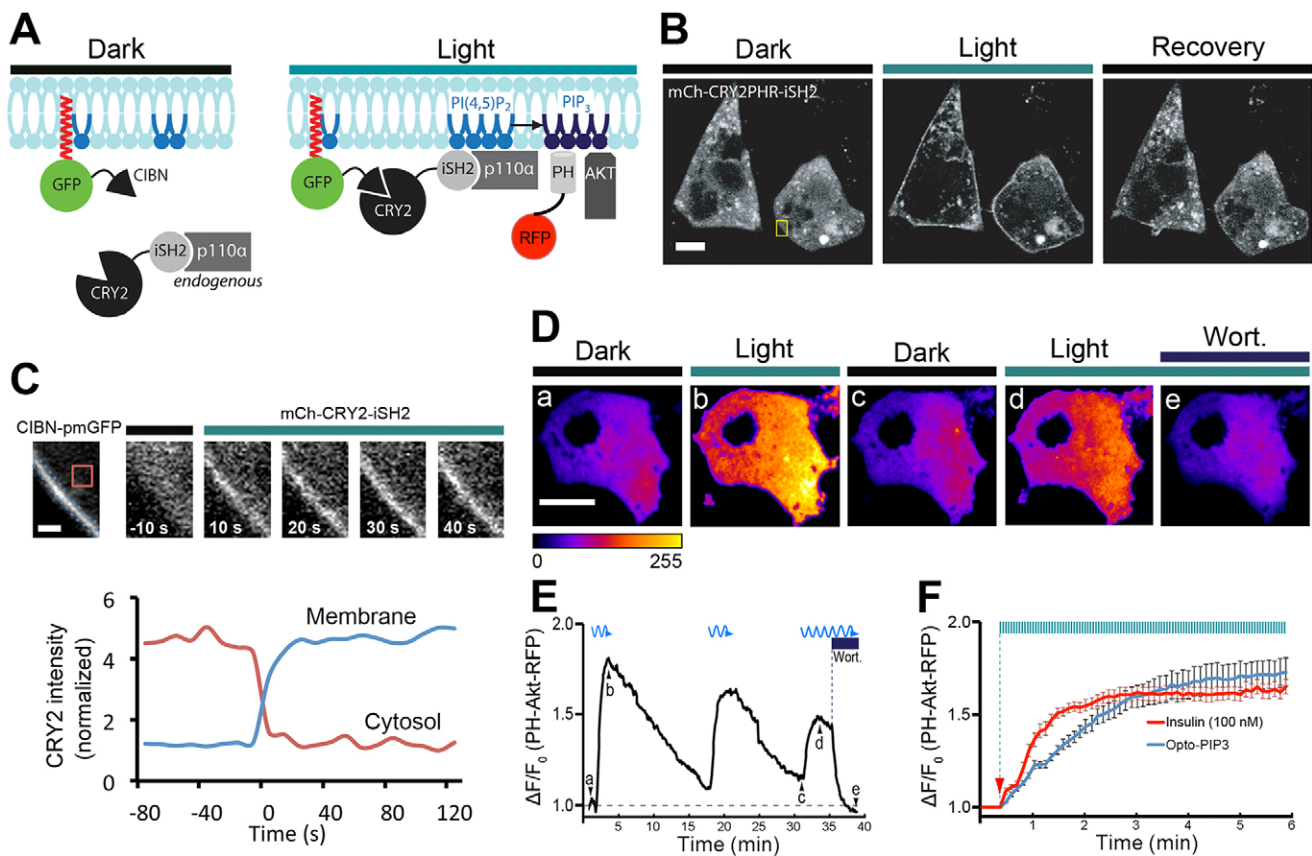
Fig. 1. Using light to control the PIP$_3$ production in 3T3-L1 adipocytes. 3T3-L1 adipocytes were electroporated with CIBN–pmGFP and mCherry–CRY2–iSH2, or with CIBN–CaaX, CRY2–iSH2 and PH-Akt–mRFP. (A) Schematic of PI3K recruitment to the plasma membrane (CIBN–pmGFP) using a fluorescent CRY2 fusion protein (mCherry–CRY2–iSH2) that constitutively binds to the endogenous PI3K catalytic subunit (p110α). Recruited PI3K converts PIP$_2$ to PIP$_3$ on the plasma membrane, which can be visualized by the PH-Akt–mRFP biosensor. (B,C) Light-triggered translocation of CRY2 fusion protein to the cell surface. Fluorescent images of CRY2 fusion protein were imaged before light activation (dark), 10 s after a 500-ms pulse of blue light (488 nm) and 1 min after pulses of blue light activation (recovery) using spinning disk confocal microscopy (B). Enlarged ROIs (yellow box in B) show the time course of CRY2 fusion protein recruitment to the plasma membrane, and the graph underneath shows quantification of mCherry–CRY2–iSH2 in the cytoplasm and at the cell surface, using the regions shown by the dotted and solid lines, respectively (C). (D–F) Light-induced production of PIP$_3$, its reversibility and sensitivity to PI3K inhibitor wortmannin (wort.). 3T3-L1 adipocytes were activated with 500-ms pulses of blue light (488 nm, 10 mW) at 5-s intervals under TIRFM illumination, and PIP$_3$ production near the cell surface was detected using 561-nm TIRFM laser beam. Selective frames of PH-Akt–mRFP images are shown in D, and corresponding time points (Da–De) are marked in real time fluorescence traces in E. The kinetics of insulin (100 nM) and Opto-PIP$_3$ induced recruitment of PH-Akt–mRFP to the cell surface are plotted in F. Arrow indicates when insulin and blue light were applied. (n=5 cells, data are mean±s.e.m.). Scale bars: 10 µm (B,D); 2 µm (C).

adipocytes were electroporated with the Opto-PIP$_3$ optogenetic module and with GLUT4–DsRed or IRAP–pHluorin. IRAP is a protein that co-traffics with GLUT4, which is tagged here, as previously described, with a pH-sensitive GFP (pHluorin) to facilitate the detection of exocytic translocation to the plasma membrane (Chen et al., 2012; Jiang et al., 2008; Stenkula et al., 2010) (see Fig. 3A and B; Movie 3). Similar to previous studies using insulin (Bai et al., 2007; Huang et al., 2007), Opto-PIP$_3$ greatly increased both GLUT4 vesicle density and the footprint of total fluorescence intensity near the cell surface, as visualized by TIRFM imaging of GLUT4–DsRed (Fig. S2). Similarly, the intensity of IRAP–pHluorin on the plasma membrane increased during light activation (Fig. 3A), and a kymograph (Fig. 3B) of the movie (Movie 3) showed a number of punctate bursts corresponding to individual vesicle fusion events. We quantified the kinetic profile of the plasma membrane signal from multiple cells that had been stimulated with either light or insulin (n=5 cells per condition). The magnitude of Opto-PIP$_3$-induced IRAP translocation to the plasma membrane was comparable to that stimulated by 100 nM insulin (~1.9 fold), and greater than that observed after stimulation with 10 nM insulin (Fig. 3C). Of note, the initial response of GLUT4

vesicle exocytosis upon Opto-PIP$_3$ activation was delayed by about ~2 min compared to the response to stimulation with 100 nM insulin. This might, in part, reflect blunted PIP$_3$ generation in Opto-PIP$_3$-stimulated cells (Fig. 1F). Insulin also acts through non-PI3K signaling pathways to trigger the initial release of GSVs to the cell surface (Belman et al., 2014; Bogan et al., 2012; Xu et al., 2011b). In control experiments, no IRAP translocation was detected in cells that had been treated with wortmannin or in those that expressed only CRY2–iSH2 (Fig. 3C). Similarly, Opto-PIP$_3$ did not induce transferrin receptor (TfR)–pHluorin exocytosis, implying that this signaling pathway selectively acts on GSVs and not on endosomes (Fig. S2D).

Akt activation is insufficient to mimic the effect of maximal insulin stimulation on GLUT4 vesicle exocytosis in 3T3-L1 adipocytes

To 'walk down' the insulin signaling pathway, we employed a similar light-induced protein heterodimerization strategy to acutely control the activity of Akt2, the key Akt isoform in GLUT4 trafficking, and to test its function in 3T3-L1 adipocytes. We designed a novel optogenetic probe, 'Opto-Akt', comprising a CIBN–CaaX 'bait'
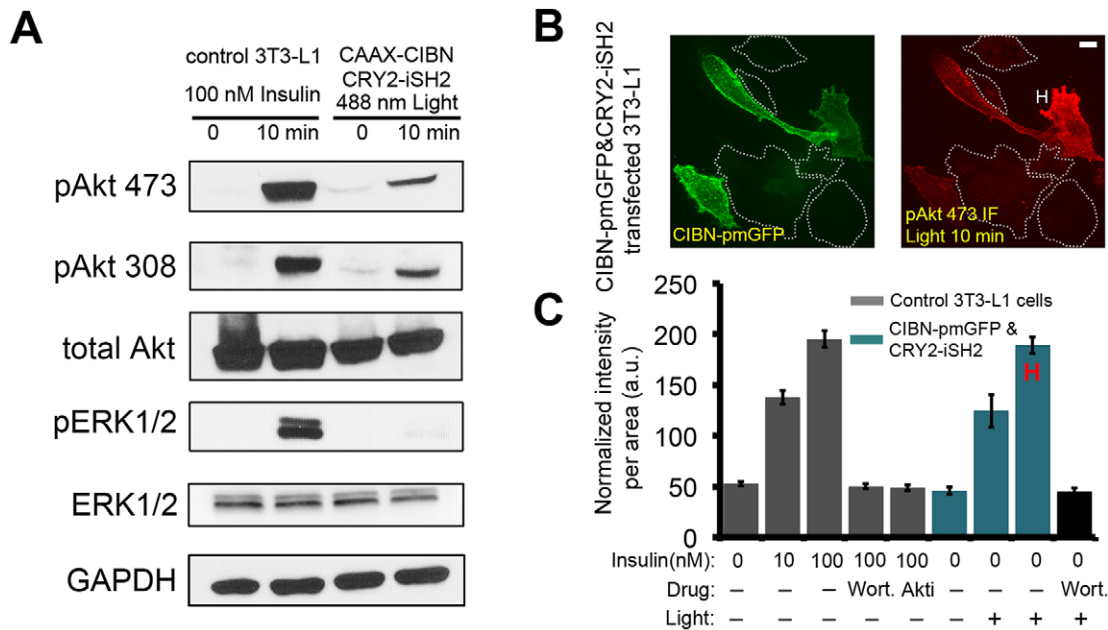
Fig. 2. Opto-PI*P*₃ activates downstream Akt phosphorylation. (A) Control 3T3-L1 adipocytes and cells that had been transfected with CIBN–CaaX and CRY2–iSH2 plasmids were treated with insulin or exposure to 488 nm LED light, respectively. Cells lysates were immunoblotted as indicated. pAkt 473 and pAkt308, Akt phosphorylated at Ser473 and Thr308, respectively; pERK1/2, phosphorylated ERK1/2. (B) Immunofluorescence staining of phosphorylated Akt (Ser473) in CIBN–pmGFP- and CRY2–iSH2-expressing adipocytes after exposure to 488-nm LED light. 'H' indicates a representative highly-responsive cell. (C) Quantification of phosphorylated Akt (at Ser473) levels in single cells. (*n*=30 cells, data are mean±s.e.m.). Scale bar: 10 µm (B).

and mCherry–CRY2–Akt 'prey'; this chimeric Akt protein can be acutely targeted to the plasma membrane in response to blue light (Fig. 4A). To test the ability of Opto-Akt2 to activate Akt signaling pathways, and to monitor the responsiveness relative to Opto-PI*P*₃, we transfected cells with either Opto-Akt constructs (mCherry–CRY2–Akt2 and CIBN–CaaX) or Opto-PI*P*₃ constructs (CRY2–iSH2 and CIBN–CaaX), and stimulated the cells with insulin or blue light (LED box). As expected, insulin triggered phosphorylation of both endogenous Akt (lower band) and mCherry–CRY2–Akt2 (upper band) at residues Thr308 and Ser473. Both sites showed a higher degree of phosphorylation with 100 nM insulin compared to 10 nM insulin, consistent with several papers showing that insulin

stimulation of Akt phosphorylation and GLUT4 translocation is dose dependent (Cheney et al., 2011; Govers et al., 2004; Kleinert et al., 2014; Martinez et al., 2010). Importantly, stimulation of Opto-Akt2 with light produced strong phosphorylation of mCherry–CRY–Akt2 at Thr308 and Ser473 (and not the endogenous Akt), whereas Opto-PI*P*₃ yielded a similar degree of responsiveness of endogenous Akt. These results support that the Opto-Akt protein is robust and functional, and can be activated by light (and insulin) on the Thr308 and Ser473 sites.

Importantly, only exogenously expressed mCherry–CRY2–Akt2 was phosphorylated at Ser473 and Thr308 after 10 min of light exposure, whereas insulin stimulated the phosphorylation of both
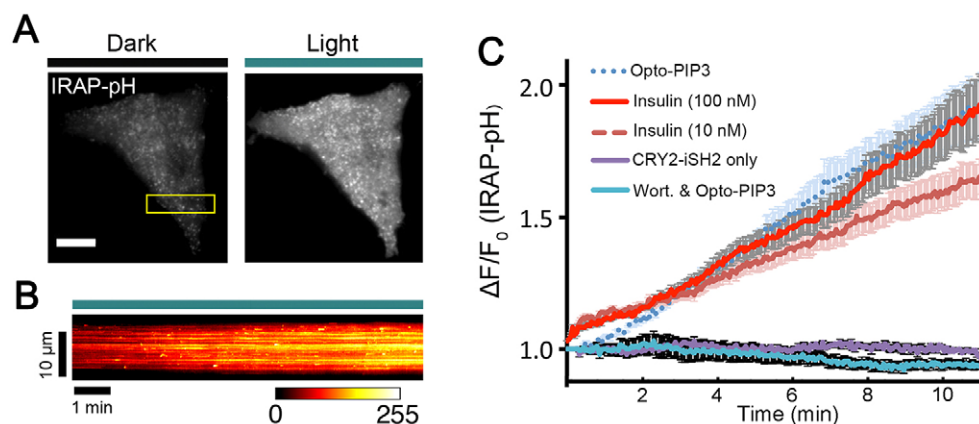

Fig. 3. Light-induced PI*P*₃ production promotes GLUT4 translocation in 3T3-L1 adipocytes. 3T3-L1 adipocytes were electroporated with CIBN–CaaX, CRY2–iSH2 and IRAP–pHluorin plasmids. The cells were activated with 500-ms pulses of blue light (488 nm, 10 mW) at 5-s intervals under TIRF illumination, and GLUT4 translocation was evaluated using IRAP–pHluorin signals on the cell surface. (A) TIRF images of a 3T3-L1 adipocyte before and after 10 min of activation with 488-nm light. (B) Kymograph image shows the dynamics of IRAP translocation to the cell surface (ROI from the box in Fig. 3A). (C) Quantification of IRAP translocation under the conditions indicated. $\Delta F/F_0$, image intensities were normalized to the intensity measured before insulin and blue light stimulation. (*n*=5 cells, data are mean± s.e.m.). Scale bar: 10 µm (A).
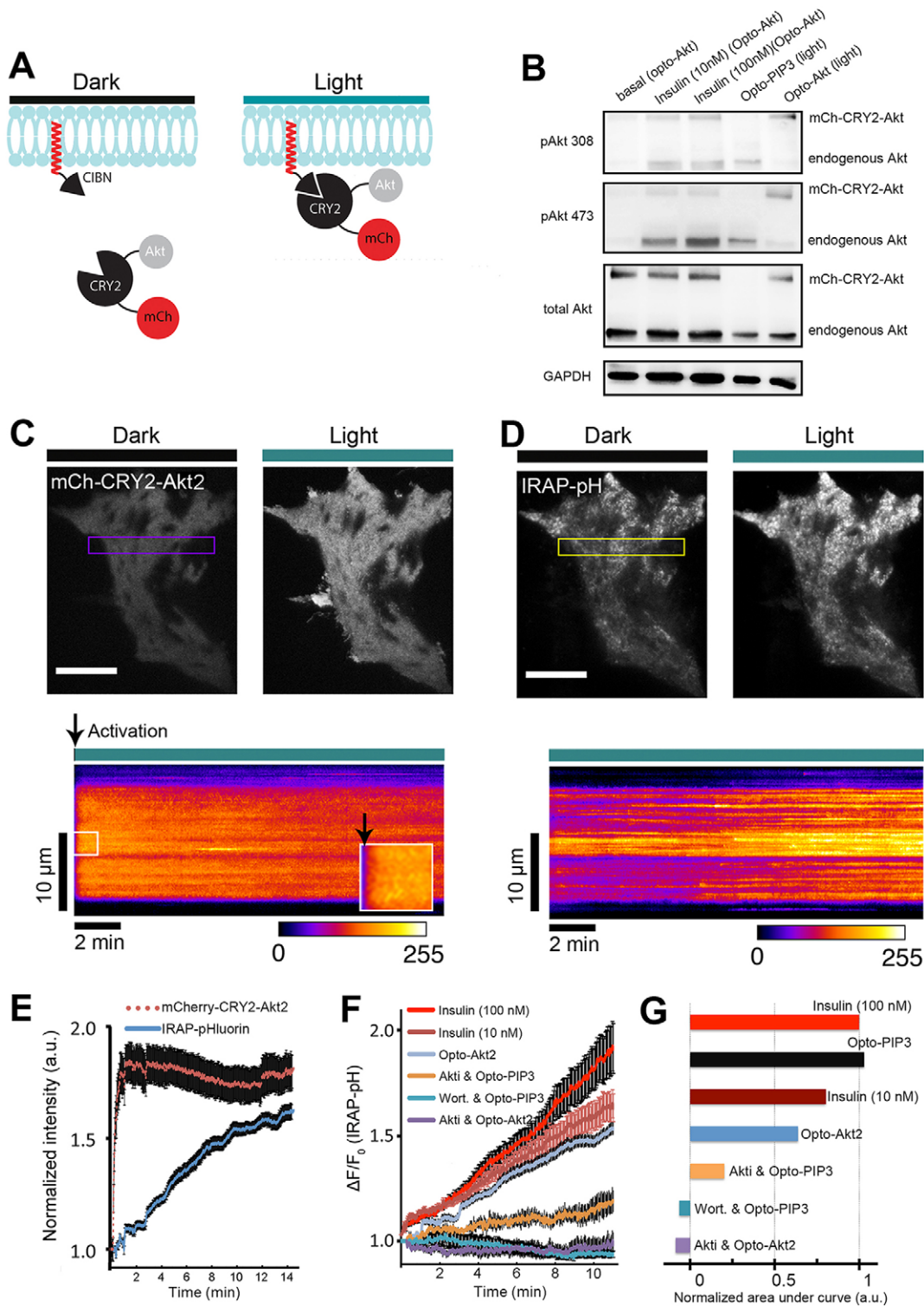
Fig. 4. Light-induced Akt relocation to the plasma membrane triggers GLUT4 translocation. (A) Schematic representation of chimeric CIBN and CRY2 constructs used in this study. (B) Light- and insulin-induced activation of mCherry–CRY2–Akt2 (mCh–CRY2–Akt). Cell lysates were immunoblotted for proteins as indicated. pAkt 473 and pAkt308, Akt phosphorylated at Ser473 and Thr308, respectively. (C) Rapid relocation of Akt fusion proteins to the cell surface after light activation. TIRF images show mCherry-tagged Akt fusion proteins before and after one pulse of blue light (488 nm, 10 mW) activation in a 3T3-L1 adipocyte. Kymograph of the boxed area is shown underneath. Arrowheads show when the light activation started. (D) Opto-Akt stimulates IRAP–pHluorin exocytosis. 3T3-L1 adipocytes were electroporated with CIBN–CaaX, mCherry–CRY2–Akt2 and IRAP–pHluorin plasmids. The cells were activated with 500-ms pulses of blue light (488 nm, 10 mW) at 5-s intervals under TIRFM illumination, and GLUT4 translocation was evaluated using pHluorin signals on the cell surface. TIRF images show IRAP–pHluorin signals before and 10 min after light activation. The kymograph of the boxed area shows the dynamics of IRAP translocation. (E) Quantification of light-induced redistribution of mCherry-tagged Akt2 fusion proteins and IRAP–pHluorin to the cell surface (n=5 cells, data are mean±s.e.m.). (F) Quantification of IRAP translocation under the conditions indicated (from top to bottom) (n=5 cells, data are mean±s.e.m.). (G) Quantification of the areas under each curve in Fig. 4F, normalized to that of the 100-nM insulin curve. Scale bars: 10 µm (C,D).

endogenous and exogenous Akt proteins (Fig. 4B). To test whether light-induced phosphorylation of exogenously expressed Akt2 was similar in magnitude to that seen upon stimulation with insulin, we used both fluorescence microscopy and immunoblotting analyses (Fig. S3). Akt phosphorylated at Ser473 was quantified by immunofluoresence in transfected and untransfected cells, and data were normalized to mCherry–CRY2–Akt2 expression using mCherry fluorescence intensity and plotted, showing that Akt phosphorylation was similar in light- and insulin-stimulated cells (Fig. S3B). Immunoblots were quantified, and they also demonstrated similar levels of Akt phosphorylation; after accounting for the 30–55% transfection efficiency, the light-induced Akt phosphorylation might even have been two- to three-fold greater than that induced by insulin (Fig. S3C). Taken together, these data confirm the selectivity and effectiveness of the Opto-Akt2 optogenetic module.

We next tested whether Opto-Akt2 stimulated GSV exocytosis in 3T3-L1 adipocytes. The cells were electroporated with CIBN–CaaX, mCherry–CRY2–Akt2 and IRAP–pHluorin. Upon blue-light exposure, we detected a rapid and strong translocation of mCherry–CRY2–Akt2 to the cell surface ($t_{1/2}$=11±3 s; mean±s.e.m.) (Fig. 4C and E); this recruitment of mCherry–CRY2–Akt2 to the cell surface was uniform (for example, see kymograph in Fig. 4C). Light-induced activation of Opto-Akt2 triggered exocytosis of IRAP–pHluorin (Fig. 4D and E), resulting in a ~1.5-fold increase in the pHluorin signal after 15 min. Recent data show that Akt1 can function redundantly with Akt2 to promote GLUT4 translocation in 3T3-L1 adipocytes (Kajno et al., 2015). To study the isoform specificity of Akt signaling using optogenetics, we used mCherry–CRY2–Akt1 (Fig. S4). Similar to the case for Akt2, we observed that Opto-Akt1 potently stimulated the exocytosis of IRAP–pHluorin, and its effect was slightly greater than that of Opto-Akt2. We observed a cumulative effect of simultaneous insulin stimulation and Opto-Akt1 activation, which was greater than the effect of Opto-Akt1 alone, on translocation of IRAP.

The use of both Opto-PIP_3 (Figs 1–3) and Opto-Akt (Fig. 4A–E; Fig. S4) provides a new opportunity to compare, directly and under similar experimental conditions, the relative importance of PIP_3 and Akt2 as downstream signaling modules in GSV translocation. Interestingly, the effect of Opto-Akt2 to stimulate IRAP translocation resembled that of 10 nM insulin, and was less effective than either 100 nM insulin or Opto-PIP_3 (Fig. 4F). Pre-treatment with Akti, an inhibitor of Akt signaling, completely blocked Akt phosphorylation and Opto-Akt2-induced IRAP translocation (Fig. 4F; Fig. S1). However, in corresponding Opto-PIP_3 experiments, Akti only partially inhibited Opto-PIP_3-induced translocation, implying that non-Akt signals act downstream of PIP_3 to promote IRAP translocation (Fig. 4F). To better illustrate these effects, we analyzed the areas under each curve in Fig. 4F and normalized the data to those upon stimulation with 100 nM insulin (Fig. 4G). We found that Opto-Akt2 triggered ~64% of maximal IRAP translocation (blue), whereas Opto-PIP_3 in the presence of Akti still had a ~20% response. In conclusion, the data show that Opto-Akt mimics the degree of the response of 10 nM insulin, which accounts for about two-thirds of the maximum insulin response (observed using 100 nM insulin). The Opto-PIP_3 response was completely abolished by the PI3K inhibitor wortmannin, whereas pharmacological inhibition of Akt was only partial.

Local recruitment of Opto-Akt controls spatial exocytosis of GLUT4

Spatial compartmentalization of signaling molecules is important for ensuring signaling specificity and proper propagation.

Optogenetic approaches permit the precise control of signaling at sub-cellular resolution (Karunarathne et al., 2015; Toettcher et al., 2011). Our previous study showed that insulin-stimulated GLUT4 exocytosis is spatially clustered (Letinic et al., 2010), suggesting that a local signal might specify where the vesicles dock and fuse. Here, we tested this hypothesis by using Opto-PIP_3 and Opto-Akt to activate signaling in a localized manner in 3T3-L1 adipocytes while monitoring the GLUT4 exocytosis response (Fig. 5).

We performed spatial photokinesis experiments in combination with TIRFM imaging, using our custom Galvo-'ring'-TIRFM–FRAP setup (Rivera-Molina and Toomre, 2013), and using the 405-nm laser line for local spatial photoactivation. To employ the Opto-Akt2 optogenetic module, 3T3-L1 adipocytes were electroporated with CIBN–CaaX, mCherry–CRY2–Akt2 and IRAP–pHluorin plasmids. Transfected cells were identified by the mCherry signal under the TIRFM (Fig. 5A, top). After a single snapshot of the IRAP–pHluorin fluorescence with TIRFM (Fig. 5C, top), to provide a basal reference image without photoactivating the cells, the cells were locally photoactivated at 405-nm using the 'fluorescence recovery after photobleaching (FRAP)–photokinesis' setting, with a ~1 µm diameter spot (green dot). As expected, CRY2–Akt2 was mobilized to the photoactivated spot and formed a smooth decaying gradient, which peaked near the photoactivation spot (Fig. 5A and B). After ~10 min of activation, another snapshot of IRAP–pHluorin was captured so as to compare the spatial distribution of IRAP–pHluorin versus the basal profile (Fig. 5C, bottom). Visually, IRAP–pHluorin mirrored the mCherry–CRY2–Akt2 distribution. To quantify these studies, circles of increasing diameters were drawn radially from the center of the activation foci (Fig. 5D), and the average intensities of mCherry–CRY2–Akt2 and IRAP–pHluorin in individual inner annular areas were calculated (n=5 cells) (Fig. 5D). As shown in Fig. 5E, the light-induced exocytosis of IRAP–pHluorin resulted in a gradient in its subsequent distribution on the cell surface. This gradient matched, within a 95% confidence band (Fig. 5F), a linear fit of the radial distribution of CRY2–Akt2. We performed similar experiments using Opto-PIP_3 to test whether PIP_3 acts locally to promote IRAP–pHluorin exocytosis. These experiments did not reveal a clear local effect of PIP_3, in contrast to the data we obtained using Opto–Akt2. In summary, these optogenetic experiments support the idea that activated Akt plays a role at or near the plasma membrane to modulate where fusion occurs.

DISCUSSION
In the present study, we applied a light-controllable tool set using Opto-PIP_3 and a new optogenetic probe, Opto-Akt, to acutely and specifically regulate PI3K and Akt signaling in time and space. These tools enable us to dissect the insulin-signaling pathway, and to decipher the relative roles of PI3K and Akt in the physiological regulation of GLUT4 translocation in 3T3-L1 adipocytes.

Optogenetics has emerged as a powerful approach to control and study physiological processes at the single-cell level (Karunarathne et al., 2015; Toettcher et al., 2011). For the first time, we employ optogenetics in adipocytes to control signaling and membrane trafficking. The light-induced heterodimerization of CRY2 and CIBN was rapid and reversible (Fig. 1), and displayed on–off rates similar to those in previous studies (Idevall-Hagren et al., 2012; Kennedy et al., 2010). Opto-PIP_3, which controls endogenous PI3K activity in a light-dependent manner, can rapidly, specifically and reversibly generate PIP_3 in adipocytes (Fig. 1). The magnitude of PIP_3 generation using Opto-PIP_3 is similar to that obtained upon
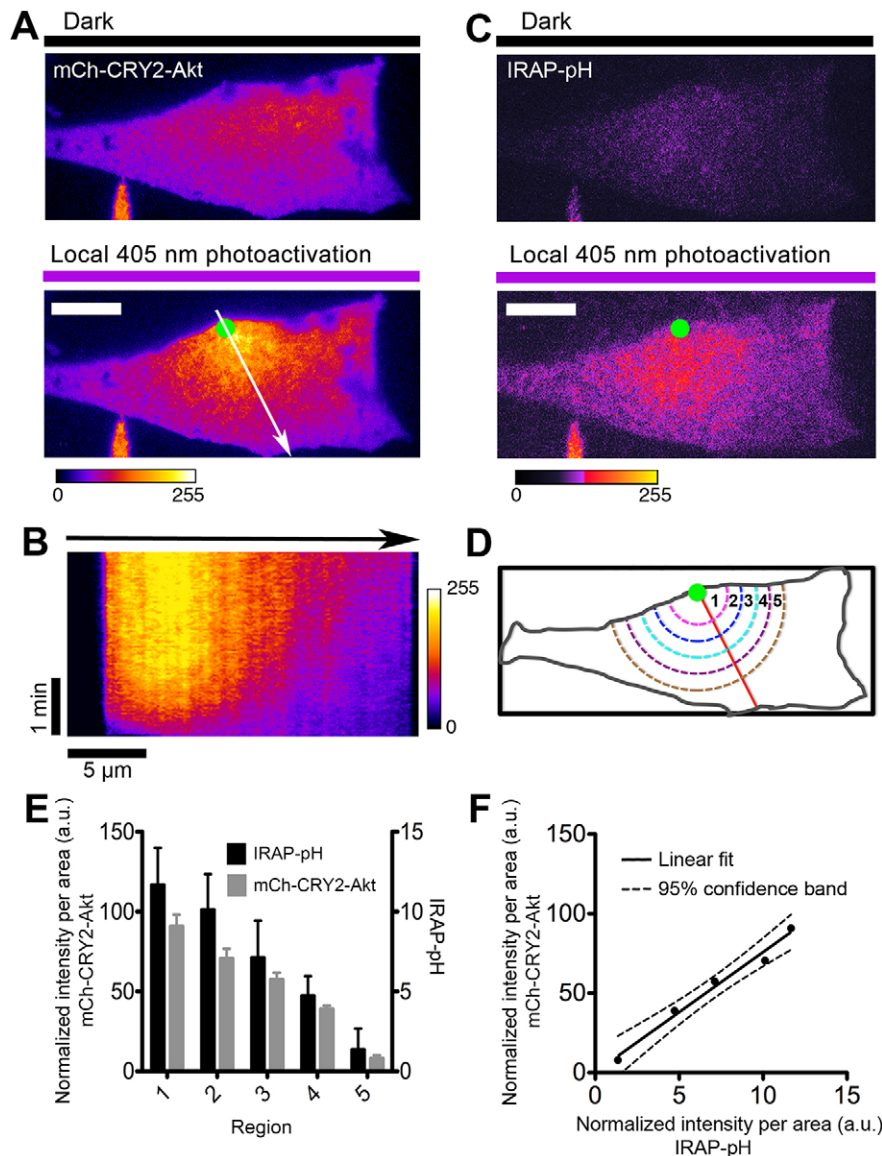
Fig. 5. Spatial control of GLUT4 vesicle exocytosis by locally confined activation of Akt in 3T3-L1 adipocytes. (A) Local recruitment of mCherry-tagged CRY2–Akt2 fusion proteins to the cell surface. The cells were activated with 500-ms pulses of UV light (405 nm, 10 mW) at 5-s intervals under FRAP–TIRFM illumination. TIRF images show mCherry–CRY2–Akt2 signals before and 10 min after FRAP activation. Green dot indicates the FRAP position. Arrow indicates the direction for kymograph (B) and spatial analysis (D). (B) Kymograph image shows the dynamics of spatial recruitment of mCherry–CRY2–Akt2 to the cell surface with 405-nm laser FRAP (single pixel line trace from Fig. 5A). (C) TIRF images of IRAP–pHluorin (IRAP–pH) signals before and 10 min after FRAP–TIRFM activation (405 nm, 10 mW). Green dot indicates the FRAP position. (D) Schematic illustration of the analysis of fluorescence distribution on the cell surface (see details in Materials and Methods). (E) Quantification of spatial distribution of mCherry-tagged CRY2–Akt2 proteins and IRAP–pH fluorescence signals (n=5 cells, data are mean±s.e.m.). (F) Linear fit shows a statistically significant correlation between light-induced confined Akt activation and its promoted spatial control of GLUT4 vesicle exocytosis, as evaluated using IRAP–pH signals on the cell surface. Scale bars: 10 µm (A,C).

insulin stimulation (Fig. 1F), implying that Opto-PIP_3 mimics insulin's effect on PI3K activation. However, the initial rates of PIP_3 production are different after insulin versus Opto-PIP_3 stimulation, which might reflect additional signals that are triggered by insulin and/or compartmentalization of PIP_2. Of note, binding of the activated insulin receptor substrate to the PI3K p85 subunit might occur in lipid microdomains, suggesting a role for compartmentalized signaling (Chang et al., 2004; Virkamäki et al., 1999).

In adipocytes, PI3K has been shown to be essential for insulin-stimulated GLUT4 translocation. Inhibition of PI3K activity with specific inhibitors – such as wortmannin – expression of dominant-negative mutants, or microinjection of blocking antibodies can completely abolish translocation (Cheatham et al., 1994; Clarke et al., 1994; Sharma et al., 1998). In contrast, overexpression of a constitutively active p110 subunit of PI3K (Katagiri et al., 1996; Martin et al., 1996; Tanti et al., 1996) or the addition of cell-permeable derivatives of PIP_3 (Sweeney et al., 2004) triggers insulin-independent GLUT4 surface translocation. Our experiments demonstrate that Opto-PIP_3 specifically activates PI3K and its downstream effector Akt, and mimics much of insulin's effect to

promote GSV exocytosis in 3T3-L1 adipocytes. Opto-PIP_3 not only recruits Akt (Fig. 1D–F), but also causes its phosphorylation at Thr308 and Ser473, two sites essential for its activation. Opto-PIP_3 bypasses other signals originating from the insulin receptor (as monitored by analyzing phosphorylated Erk) and, with the exception of a slight initial delay, promotes GLUT4 exocytosis in a manner similar to that observed with 100 nM insulin (Fig. 3). As noted, the initial delay in the exocytosis response was consistent with insulin action through a non-PI3K signaling pathway, the effect of which might be minimized in 3T3-L1 adipocytes compared to in primary adipocytes (Baumann et al., 2000; Belman et al., 2014; Bogan et al., 2012; Chang et al., 2007; Muretta et al., 2008; Xu et al., 2011b). Taken together, the data reemphasize the central role of PI3K as a major effector connecting insulin signaling with vesicle trafficking.

Akt, which has three isoforms in mammals, is another crucial node in insulin signaling; however, until now there have been no optogenetic tools to control its activity spatially and temporally. Knockout and knockdown studies have demonstrated that Akt2 is the main isoform required for insulin-regulated GLUT4 trafficking and glucose uptake (Bae et al., 2003; Cho et al., 2001a; Kohn et al., 1996).

Possibly, this isoform specificity results from effects on subcellular localization, and the phosphorylation of Akt specifically at the plasma membrane is proposed to mediate the main effect of insulin on translocation of GLUT4 (Gonzalez and McGraw, 2009; Ng et al., 2010a). By using light to selectively and rapidly activate Akt2 at the plasma membrane in 3T3-L1 adipocytes, we show that although Akt2 plays a major role in stimulating IRAP and GLUT4 translocation, it is not as effective as either 100 nM insulin or optogenetic production of PIP_3 (Fig. 4F; Fig. S2). We obtained similar results using light-induced activation of Akt1, and further showed that concurrent insulin addition had an additive effect on the translocation of IRAP (Fig. S4). Our conclusion that Akt signaling accounts for only two-thirds of the insulin response differs markedly with the interpretation of previous work (Ng et al., 2008), which concludes that Akt2 activation is sufficient to stimulate GLUT4 translocation to an extent similar to that of insulin. Although that previous study manipulated Akt acutely using chemical genetics rather than light, a key distinction with our work is that the maximal insulin dose that was tested in that previous study was 10 nM. A second distinction of our data is that the optogenetic activation is considerably faster than the dimer-inducing chemical used previously (Ng et al., 2008), which is limited by the prolonged diffusion time of the added compounds, as well as by low reversibility and spatial precision. Apart from the 2-min initial lag, the kinetics of IRAP translocation induced by Opto-Akt2 were very similar to that induced by 10 nM insulin. By contrast, in the chemical-genetic FKBP–FRB heterodimerization system [comprising FKBP and the rapamycin-binding domain of mTOR (FRB)], translocation was approximately twice as slow. It remains unclear why the kinetics are so different, but possibilities include technical issues, such as diffusion of the chemical-genetic drug or slower heterodimerization. Third, our approach used a real-time assay in living cells, which allowed us to detect differences in the response during the first two minutes (these would have been missed by a fixed timepoint analysis at 5-min intervals). The key ramification of our experiments is that PI3K and Akt do not play equivalent roles in GLUT4 translocation. Rather, our data support the idea that PI3K activates a broader range of signals, in addition to Akt. Our results are consistent with older data arguing the existence of Akt-independent actions of PI3K (Gonzalez and McGraw, 2006). Other signaling pathways, such as PI3K-dependent activation of the exocyst complex (Chen et al., 2011) and atypical protein kinase C pathways (Kanzaki et al., 2004; Liu et al., 2010; Sajan et al., 2014a,b) might be activated in adipocytes, but these have not been well appreciated. Particularly in muscle cells, PI3K stimulates Rac1 signaling, and this is required together with Akt to promote GLUT4 translocation and glucose uptake (Chiu et al., 2011; Klip et al., 2014; Sylow et al., 2014; Ueda et al., 2010). The Rac1 pathway is likely to act in adipocytes as well (Balamatsias et al., 2011; Tsuchiya et al., 2015). Our data support an important role for these and, possibly, other pathways.

Although the initial delay in Opto-PIP_3-induced IRAP translocation might result from the kinetics of PIP_3 production, which were slower compared to those induced by insulin, another possibility is that the initial insulin response results in part from PI3K-independent signaling. Such pathways are not stimulated by Opto-PIP_3. We have previously shown that GSV cargos translocate to the cell surface in two distinct types of vesicles (Xu et al., 2011b). Smaller vesicles, characteristic of GSVs, were the main carrier at 3–6 min after insulin addition, whereas GSV cargos arrived at the plasma membrane in larger vesicles, likely to be derived from endosomes, both at >15 min after insulin addition and (at a slower rate) in unstimulated cells. Data here support the idea that translocation of the GSVs might not be fully activated by Opto-

PIP_3, consistent with the observation that these vesicles are regulated by a PI3K-independent signaling pathway through TC10α to stimulate endoproteolytic cleavage of TUG proteins (Bogan et al., 2012; Xu et al., 2011b). Release of TUG-bound GLUT4-containing vesicles can fully mimic the effect of acute insulin stimulation in 3T3-L1 adipocytes (Xu et al., 2011b; Yu et al., 2007) and in skeletal muscle (Löffler et al., 2013). This pathway is modulated by nutritional effects, through TUG acetylation (Belman et al., 2015), and coordinates vasopressin action, and probably energy expenditure, with the stimulation of glucose uptake in vivo (Habtemichael et al., 2015; Löffler et al., 2013). Different assessments of the importance of non-PI3K signaling might reflect the use of 3T3-L1 adipocytes, which are an imperfect model system, as well as variation in the methods used by different labs (Govers et al., 2004; Martin et al., 2006; Muretta et al., 2008). More broadly, data presented here highlight the limitations, as well as the strengths, of reconstitution studies to test the sufficiency of individual signaling pathways. Effects that might appear to be minor in tests of sufficiency might actually be quite important when assessed by tests of necessity.

The application of Opto-Akt also allowed us to selectively activate Akt at a specific region of cell and to test how confined Akt signaling affects GLUT4 exocytosis. We demonstrated that Akt provides the fidelity of spatial release of GLUT4 on the cell surface, and our findings support previous work that Akt signaling at the plasma membrane is required for the last step of GLUT4 exocytosis (Koumanov et al., 2005). Moreover, a downstream target of Akt, AS160, is mobilized to the plasma membrane and regulates GLUT4 vesicle exocytosis (Tan et al., 2012). Therefore, it is conceivable that locally activated Akt might recruit AS160 and its downstream Rab proteins, as well as the exocyst complex (Chen et al., 2011), to control the spatial release of GLUT4 into the plasma membrane. Of note, data presented here support the idea that there is a local permanence of activated Akt effectors, such as AS160, and its targets, such as Rab10 and Rab13, which mediate vesicle tethering, docking and fusion at the plasma membrane (Chen et al., 2012; Sun et al., 2010). Understanding precisely how these effectors act will require further investigation.

The combined use of Opto-PIP_3 and Opto-Akt holds considerable potential for use in other biological systems to elucidate and dissect PI3K–Akt signaling nodes. Clearly PI3K and Akt signaling can be tightly coupled, whereas it is often assumed that they are in single unique 'PI3K–Akt' pathway (Porta et al., 2014), but this has not been thoroughly tested. As demonstrated herein, the use of multiple optogenetic signals allows quantitative spatial-temporal testing of these nodes and, with precise light dose control, even putative tuning of the activation of PI3K and Akt signaling. Moreover, Opto-Akt as a new light-controllable signaling molecule should enable study of isoform-specific effects of Akt in various diseases, such as cancer and diabetes, as well as probing for unique downstream targets.

In summary, our study is the first to use optogenetics in adipocytes to investigate the mechanism of insulin signaling and GLUT4 translocation. We demonstrate that this optogenetic approach permits the control of individual insulin signaling molecules acutely and with spatial precision. We used these novel tools to dissect the roles of PI3K and Akt molecules in GLUT4 trafficking in 3T3-L1 adipocytes. The data support a major regulatory role of PI3K and imply that downstream targets other than Akt have important and under-appreciated roles in the regulation of glucose uptake. Finally, we identify a new function of Akt in the spatial regulation of GLUT4 vesicle exocytosis in 3T3-

L1 adipocytes. Extension of this approach should be broadly applicable to elucidate mechanisms of PI3K–Akt signal transduction in other diverse areas of biology.

MATERIALS AND METHODS

Plasmids and reagents

CIBN–pmGFP, CIBN–CaaX, mCherry–CRY2–iSH2, CRY2–iSH2 and PH-Akt–mRFP plasmids were generated as described previously (Idevall-Hagren et al., 2012). HA–GLUT4–GFP and IRAP–pHluorin plasmids were provided by Dr J. Zimmerberg (NIH) (Stenkula et al., 2010). The mCherry–CRY2–Akt2 and mCherry–CRY2–Akt1 plasmids were generated by fusing the full-length human *Akt2* and *Akt1* cDNAs to the C-terminus of mCherry–CRY2. Antibodies were purchased from Cell Signaling. All other chemicals used in this study were purchased from Sigma-Aldrich.

Cell culture and transfection

3T3-L1 fibroblasts were cultured and differentiated as described previously (Xu et al., 2011b). After 8–10 days of differentiation, 3T3-L1 mature adipocytes were electroporated using an Amaxa Nucleofector instrument in a 0.1-ml transfection solution 'L' containing two or three of the above plasmids (2–4 μg total plasmid DNA per transfection).

Immunostaining and biochemical methods

Immunofluorescence cell staining was performed as described previously (Xu et al., 2007). 3T3-L1 adipocytes were fixed with 4% paraformaldehyde in PBS for 10 min at room temperature. Cells were permeabilized with 0.1% Triton X-100 for 5 min, and blocked with 1% BSA and 3% normal goat serum in PBS for 45 min. Total Akt phosphorylation was detected using either rabbit anti-phospho-Akt at Ser473 or anti-phospho-Akt at Thr308 antibodies (1:200 dilution; catalog numbers 4060 and 13038, respectively; Cell Signaling) followed by Cy3-conjugated anti-rabbit IgG (1:200 dilution). Finally, the cells were washed, mounted and imaged with a spinning disk confocal microscope.

Immunoblotting was performed as described previously (Xu et al., 2011b). 3T3-L1 adipocytes or adipocytes that had been transiently electroporated with optogenetic modules were stimulated with 100 nM insulin for 10 min or exposed to 488 nm LED light for 10 min. Cells were washed in cold PBS and scraped in ice-cold RIPA lysis buffer containing protease and phosphatase inhibitors (Roche). The cell lysates were passed through a 25-gauge syringe eight times and centrifuged for 15 min at 12,000 *g* at 4°C. Supernatants were recovered, and equal amounts of protein (determined using BCA assay) in each sample were analyzed by SDS-PAGE and immunoblotting.

Live-cell imaging

Cells were cultured on glass-bottomed 35-mm MatTek dishes and imaged 15–20 h after transfection. Before imaging, cells were serum starved for ~2 h, then imaged in KRH buffer, pH 7.4, containing 125 mM NaCl, 5 mM KCl, 1.3 mM $CaCl_2$, 1.2 mM $MgSO_4$, 20 mM D-glucose, 25 mM Hepes and 0.2% bovine serum albumin. Cells were kept in an Air-therm temperature-regulated environmental box at 37°C throughout the experiments.

A Yokagawa-type spinning disk confocal microscope system was used for fast live-cell imaging (PerkinElmer). The system was mounted onto an inverted Olympus IX-71 microscope, equipped with a 1 Kb×1 Kb EM CCD camera (Hamamatsu Photonics). A 488-nm laser line was used to induce dimerization between CIBN and CRY2 or to image GFP-tagged proteins, whereas a 561-nm laser line was used to image mCherry- or mRFP-tagged proteins. Images were acquired under the control of Volocity software at 0.2 Hz with exposure times in the 100–500 ms range.

The TIRFM setup was based on an Olympus IX-70 microscope, equipped with 405-, 488- and 568-nm laser lines, a 60×1.49 NA TIRF objective (Olympus) and an EMCCD camera (iXon887; Andor Technology). The 488-nm laser line was used to induce CIBN and CRY2 protein heterodimerization, and the 568-nm laser line was used to image mCherry- or mRFP-tagged proteins. Images were acquired under the control of Andor iQ software at 0.2–0.5 Hz with exposure times in the rage

of 200–500 ms. FRAP–TIRFM experiments were performed as described previously (Rivera-Molina and Toomre, 2013). Control 3T3-L1 cells were imaged in the basal state for a few minutes before insulin was added, similar to our previous report (Xu et al., 2011b). For the cells that had been transfected with the optogenetic module, activation of the optogenetic module was performed at the start of imaging because the pHluorin channel for imaging would otherwise dimerize the optogenetic constructs independently. For FRAP analyses of a region of interest (ROI), the 405-nm laser line was used together with custom-written software. To limit light scattering, FRAP was performed with a 100-ms exposure, followed by TIRF imaging of mCherry-tagged proteins using a 568-nm laser line. The FRAP and TIRFM modes were cycled every 5 s, for a total of 10–15 min. Two TIRFM images were taken of the IRAP–pHluorin-transfected cells before and after the FRAP–TIRFM experiments for comparison of the fluorescence distribution, using the 488-nm laser line. The cells were exposed to the 488-nm laser for as short a time as possible, in order to minimize global activation.

Image analysis and statistics

Stacks of time-lapse images were processed and analyzed using ImageJ 1.45 s (National Institutes of Health). Images were prepared with Photoshop (Adobe). Movies were compressed with QuickTime Pro (Apple) using a H.264 algorithm. Unless otherwise indicated, all data are presented as the mean±s.e.m. and were analyzed using a Student's *t*-test.

Competing interests

The authors declare no competing or financial interests.

Author contributions

Y.X., J.S.B. and D.T. designed research; Y.X., D.N. and J.F. performed research; Y.X., J.S.B. and D.T. analyzed data and wrote the paper.

Supplementary information

Supplementary information available online at
http://jcs.biologists.org/lookup/suppl/doi:10.1242/jcs.174805/-/DC1

References

Bae, S. S., Cho, H., Mu, J. and Birnbaum, M. J. (2003). Isoform-specific regulation of insulin-dependent glucose uptake by Akt/protein kinase B. *J. Biol. Chem.* **278**, 49530-49536.

Bai, L., Wang, Y., Fan, J., Chen, Y., Ji, W., Qu, A., Xu, P., James, D. E. and Xu, T. (2007). Dissecting multiple steps of GLUT4 trafficking and identifying the sites of insulin action. *Cell Metab.* **5**, 47-57.

Balamatsias, D., Kong, A. M., Waters, J. E., Sriratana, A., Gurung, R., Bailey, C. G., Rasko, J. E. J., Tiganis, T., Macaulay, S. L. and Mitchell, C. A. (2011). Identification of P-Rex1 as a novel Rac1-guanine nucleotide exchange factor (GEF) that promotes actin remodeling and GLUT4 protein trafficking in adipocytes. *J. Biol. Chem.* **286**, 43229-43240.

Baumann, C. A., Ribon, V., Kanzaki, M., Thurmond, D. C., Mora, S., Shigematsu, S., Bickel, P. E., Pessin, J. E. and Saltiel, A. R. (2000). CAP defines a second signalling pathway required for insulin-stimulated glucose transport. *Nature* **407**, 202-207.

Belman, J. P., Habtemichael, E. N. and Bogan, J. S. (2014). A proteolytic pathway that controls glucose uptake in fat and muscle. *Rev. Endocr. Metab. Disord.* **15**, 55-66.

Belman, J. P., Bian, R. R., Habtemichael, E. N., Li, D. T., Jurczak, M. J., Alcázar-Román, A., McNally, L. J., Shulman, G. I. and Bogan, J. S. (2015). Acetylation of TUG protein promotes the accumulation of GLUT4 glucose transporters in an insulin-responsive intracellular compartment. *J. Biol. Chem.* 290, 4447-4463.

Bogan, J. S. (2012). Regulation of glucose transporter translocation in health and diabetes. *Annu. Rev. Biochem.* 81, 507-532.

Bogan, J. S., Rubin, B. R., Yu, C., Loffler, M. G., Orme, C. M., Belman, J. P., McNally, L. J., Hao, M. and Cresswell, J. A. (2012). Endoproteolytic cleavage of TUG protein regulates GLUT4 glucose transporter translocation. *J. Biol. Chem.* 287, 23932-23947.

Chang, L., Chiang, S. H. and Saltiel, A. R. (2004). Insulin signaling and the regulation of glucose transport. *Mol. Med.* 10, 65-71.

Chang, L., Chiang, S.-H. and Saltiel, A. R. (2007). TC10alpha is required for insulin-stimulated glucose uptake in adipocytes. *Endocrinology* 148, 27-33.

Cheatham, B., Vlahos, C. J., Cheatham, L., Wang, L., Blenis, J. and Kahn, C. R. (1994). Phosphatidylinositol 3-kinase activation is required for insulin stimulation of pp70 S6 kinase, DNA synthesis, and glucose transporter translocation. *Mol. Cell. Biol.* 14, 4902-4911.

Chen, X.-W., Leto, D., Xiong, T., Yu, G., Cheng, A., Decker, S. and Saltiel, A. R. (2011). A Ral GAP complex links PI 3-kinase/Akt signaling to RalA activation in insulin action. *Mol. Biol. Cell* 22, 141-152.

Chen, Y., Wang, Y., Zhang, J., Deng, Y., Jiang, L., Song, E., Wu, X. S., Hammer, J. A., Xu, T. and Lippincott-Schwartz, J. (2012). Rab10 and myosin-Va mediate insulin-stimulated GLUT4 storage vesicle translocation in adipocytes. *J. Cell Biol.* 198, 545-560.

Cheney, L., Hou, J. C., Morrison, S., Pessin, J. and Steigbigel, R. T. (2011). Nef inhibits glucose uptake in adipocytes and contributes to insulin resistance in human immunodeficiency virus type I infection. *J. Infect Dis.* 203, 1824-1831.

Chiang, S.-H., Baumann, C. A., Kanzaki, M., Thurmond, D. C., Watson, R. T., Neudauer, C. L., Macara, I. G., Pessin, J. E. and Saltiel, A. R. (2001). Insulin-stimulated GLUT4 translocation requires the CAP-dependent activation of TC10. *Nature* 410, 944-948.

Chiu, T. T., Jensen, T. E., Sylow, L., Richter, E. A. and Klip, A. (2011). Rac1 signalling towards GLUT4/glucose uptake in skeletal muscle. *Cell. Signal.* 23, 1546-1554.

Cho, H., Mu, J., Kim, J. K., Thorvaldsen, J. L., Chu, Q., Crenshaw, E. B., III, Kaestner, K. H., Bartolomei, M. S., Shulman, G. I. and Birnbaum, M. J. (2001a). Insulin resistance and a diabetes mellitus-like syndrome in mice lacking the protein kinase Akt2 (PKBbeta). *Science* 292, 1728-1731.

Cho, H., Thorvaldsen, J. L., Chu, Q., Feng, F. and Birnbaum, M. J. (2001b). Akt1/PKBalpha is required for normal growth but dispensable for maintenance of glucose homeostasis in mice. *J. Biol. Chem.* 276, 38349-38352.

Clarke, J. F., Young, P. W., Yonezawa, K., Kasuga, M. and Holman, G. D. (1994). Inhibition of the translocation of GLUT1 and GLUT4 in 3T3-L1 cells by the phosphatidylinositol 3-kinase inhibitor, wortmannin. *Biochem. J.* 300, 631-635.

Farese, R. V., Sajan, M. P., Yang, H., Li, P., Mastorides, S., Gower, W. R., Jr, Nimal, S., Choi, C. S., Kim, S., Shulman, G. I. et al. (2007). Muscle-specific knockout of PKC-lambda impairs glucose transport and induces metabolic and diabetic syndromes. *J. Clin. Invest.* 117, 2289-2301.

Gautier, A., Gauron, C., Volovitch, M., Bensimon, D., Jullien, L. and Vriz, S. (2014). How to control proteins with light in living systems. *Nat. Chem. Biol.* 10, 533-541.

Gonzalez, E. and McGraw, T. E. (2006). Insulin signaling diverges into Akt-dependent and -independent signals to regulate the recruitment/docking and the fusion of GLUT4 vesicles to the plasma membrane. *Mol. Biol. Cell* 17, 4484-4493.

Gonzalez, E. and McGraw, T. E. (2009). Insulin-modulated Akt subcellular localization determines Akt isoform-specific signaling. *Proc. Natl. Acad. Sci. USA* 106, 7004-7009.

Govers, R., Coster, A. C. F. and James, D. E. (2004). Insulin increases cell surface GLUT4 levels by dose dependently discharging GLUT4 into a cell surface recycling pathway. *Mol. Cell. Biol.* 24, 6456-6466.

Habtemichael, E. N., Alcázar-Román, A., Rubin, B. R., Grossi, L. R., Belman, J. P., Julca, O., Löffler, M. G., Li, H., Chi, N.-W., Samuel, V. T. et al. (2015). Coordinated regulation of vasopressin inactivation and glucose uptake by action of TUG protein in muscle. *J. Biol. Chem.* 290, 14454-14461.

Huang, S., Lifshitz, L. M., Jones, C., Bellve, K. D., Standley, C., Fonseca, S., Corvera, S., Fogarty, K. E. and Czech, M. P. (2007). Insulin stimulates membrane fusion and GLUT4 accumulation in clathrin coats on adipocyte plasma membranes. *Mol. Cell. Biol.* 27, 3456-3469.

Idevall-Hagren, O., Dickson, E. J., Hille, B., Toomre, D. K. and De Camilli, P. (2012). Optogenetic control of phosphoinositide metabolism. *Proc. Natl. Acad. Sci. USA* 109, E2316-E2323.

Jiang, Z. Y., Zhou, Q. L., Coleman, K. A., Chouinard, M., Boese, Q. and Czech, M. P. (2003). Insulin signaling through Akt/protein kinase B analyzed by small interfering RNA-mediated gene silencing. *Proc. Natl. Acad. Sci. USA* 100, 7569-7574.

Jiang, L., Fan, J., Bai, L., Wang, Y., Chen, Y., Yang, L., Chen, L. and Xu, T. (2008). Direct quantification of fusion rate reveals a distal role for AS160 in insulin-stimulated fusion of GLUT4 storage vesicles. *J. Biol. Chem.* 283, 8508-8516.

Kahn, B. B. and Flier, J. S. (2000). Obesity and insulin resistance. *J. Clin. Invest.* 106, 473-481.

Kajno, E., McGraw, T. E. and Gonzalez, E. (2015). Development of a new model system to dissect isoform specific Akt signalling in adipocytes. *Biochem. J.* 468, 425-434.

Kanzaki, M., Mora, S., Hwang, J. B., Saltiel, A. R. and Pessin, J. E. (2004). Atypical protein kinase C (PKCzeta/lambda) is a convergent downstream target of the insulin-stimulated phosphatidylinositol 3-kinase and TC10 signaling pathways. *J. Cell Biol.* 164, 279-290.

Karunarathne, W. K. A., O'Neill, P. R. and Gautam, N. (2015). Subcellular optogenetics - controlling signaling and single-cell behavior. *J. Cell Sci.* 128, 15-25.

Katagiri, H., Asano, T., Ishihara, H., Inukai, K., Shibasaki, Y., Kikuchi, M., Yazaki, Y. and Oka, Y. (1996). Overexpression of catalytic subunit p110alpha of phosphatidylinositol 3-kinase increases glucose transport activity with translocation of glucose transporters in 3T3-L1 adipocytes. *J. Biol. Chem.* 271, 16987-16990.

Katome, T., Obata, T., Matsushima, R., Masuyama, N., Cantley, L. C., Gotoh, Y., Kishi, K., Shiota, H. and Ebina, Y. (2003). Use of RNA interference-mediated gene silencing and adenoviral overexpression to elucidate the roles of AKT/protein kinase B isoforms in insulin actions. *J. Biol. Chem.* 278, 28312-28323.

Kennedy, M. J., Hughes, R. M., Peteya, L. A., Schwartz, J. W., Ehlers, M. D. and Tucker, C. L. (2010). Rapid blue-light–mediated induction of protein interactions in living cells. *Nat. Methods* 7, 973-975.

Kleinert, M., Sylow, L., Fazakerley, D. J., Krycer, J. R., Thomas, K. C., Oxbøll, A.-J., Jordy, A. B., Jensen, T. E., Yang, G., Schjerling, P. et al. (2014). Acute mTOR inhibition induces insulin resistance and alters substrate utilization in vivo. *Mol. Metab.* 3, 630-641.

Klip, A., Sun, Y., Chiu, T. T. and Foley, K. P. (2014). Signal transduction meets vesicle traffic: the software and hardware of GLUT4 translocation. *Am. J. Physiol. Cell Physiol.* 306, C879-C886.

Kohn, A. D., Summers, S. A., Birnbaum, M. J. and Roth, R. A. (1996). Expression of a constitutively active Akt Ser/Thr kinase in 3T3-L1 adipocytes stimulates glucose uptake and glucose transporter 4 translocation. *J. Biol. Chem.* 271, 31372-31378.

Koumanov, F., Jin, B., Yang, J. and Holman, G. D. (2005). Insulin signaling meets vesicle traffic of GLUT4 at a plasma-membrane-activated fusion step. *Cell Metab.* 2, 179-189.

Letinic, K., Sebastian, R., Barthel, A. and Toomre, D. (2010). Deciphering subcellular processes in live imaging datasets via dynamic probabilistic networks. *Bioinformatics* 26, 2029-2036.

Leto, D. and Saltiel, A. R. (2012). Regulation of glucose transport by insulin: traffic control of GLUT4. *Nat. Rev. Mol. Cell Biol.* 13, 383-396.

Liu, L.-Z., Cheung, S. C. K., Lan, L.-L., Ho, S. K. S., Chan, J. C. N. and Tong, P. C. Y. (2010). The pivotal role of protein kinase C zeta (PKCzeta) in insulin- and AMP-activated protein kinase (AMPK)-mediated glucose uptake in muscle cells. *Cell. Signal.* 22, 1513-1522.

Löffler, M. G., Birkenfeld, A. L., Philbrick, K. M., Belman, J. P., Habtemichael, E. N., Booth, C. J., Castorena, C. M., Choi, C. S., Jornayvaz, F. R., Gassaway, B. M. et al. (2013). Enhanced fasting glucose turnover in mice with disrupted action of TUG protein in skeletal muscle. *J. Biol. Chem.* 288, 20135-20150.

Martin, S. S., Haruta, T., Morris, A. J., Klippel, A., Williams, L. T. and Olefsky, J. M. (1996). Activated phosphatidylinositol 3-kinase is sufficient to mediate actin rearrangement and GLUT4 translocation in 3T3-L1 adipocytes. *J. Biol. Chem.* 271, 17605-17608.

Martin, O. J., Lee, A. and McGraw, T. E. (2006). GLUT4 distribution between the plasma membrane and the intracellular compartments is maintained by an insulin-modulated bipartite dynamic mechanism. *J. Biol. Chem.* 281, 484-490.

Martinez, L., Berenguer, M., Bruce, M. C., Le Marchand-Brustel, Y. and Govers, R. (2010). Rosiglitazone increases cell surface GLUT4 levels in 3T3-L1 adipocytes through an enhancement of endosomal recycling. *Biochem. Pharmacol.* 79, 1300-1309.

McCurdy, C. E. and Cartee, G. D. (2005). Akt2 is essential for the full effect of calorie restriction on insulin-stimulated glucose uptake in skeletal muscle. *Diabetes* 54, 1349-1356.

Muretta, J. M., Romenskaia, I. and Mastick, C. C. (2008). Insulin releases Glut4 from static storage compartments into cycling endosomes and increases the rate constant for Glut4 exocytosis. *J. Biol. Chem.* 283, 311-323.

Ng, Y., Ramm, G., Lopez, J. A. and James, D. E. (2008). Rapid activation of Akt2 is sufficient to stimulate GLUT4 translocation in 3T3-L1 adipocytes. *Cell Metab.* 7, 348-356.

Ng, Y., Ramm, G., Burchfield, J. G., Coster, A. C. F., Stockli, J. and James, D. E. (2010a). Cluster analysis of insulin action in adipocytes reveals a key role for Akt at the plasma membrane. *J. Biol. Chem.* 285, 2245-2257.

Ng, Y., Ramm, G. and James, D. E. (2010b). Dissecting the mechanism of insulin resistance using a novel heterodimerization strategy to activate Akt. *J. Biol. Chem.* 285, 5232-5239.

Pathak, G. P., Vrana, J. D. and Tucker, C. L. (2013). Optogenetic control of cell function using engineered photoreceptors. *Biol. Cell* 105, 59-72.

Porta, C., Paglino, C. and Mosca, A. (2014). Targeting PI3K/Akt/mTOR Signaling in Cancer. *Front. Oncol.* **4**, 64.

Rivera-Molina, F. and Toomre, D. (2013). Live-cell imaging of exocyst links its spatiotemporal dynamics to various stages of vesicle fusion. *J. Cell Biol.* **201**, 673-680.

Sajan, M. P., Ivey, R. A., III, Lee, M., Mastorides, S., Jurczak, M. J., Samuels, V. T., Shulman, G. I., Braun, U., Leitges, M. and Farese, R. V. (2014a). PKClambda haploinsufficiency prevents diabetes by a mechanism involving alterations in hepatic enzymes. *Mol. Endocrinol.* **28**, 1097-1107.

Sajan, M. P., Jurzak, M. J., Samuels, V. T., Shulman, G. I., Braun, U., Leitges, M. and Farese, R. V. (2014b). Impairment of insulin-stimulated glucose transport and ERK activation by adipocyte-specific knockout of PKC-lambda produces a phenotype characterized by diminished adiposity and enhanced insulin suppression of hepatic gluconeogenesis. *Adipocyte* **3**, 19-29.

Saltiel, A. R. and Pessin, J. E. (2002). Insulin signaling pathways in time and space. *Trends Cell Biol.* **12**, 65-71.

Sharma, P. M., Egawa, K., Huang, Y., Martin, J. L., Huvar, I., Boss, G. R. and Olefsky, J. M. (1998). Inhibition of phosphatidylinositol 3-kinase activity by adenovirus-mediated gene transfer and its effect on insulin action. *J. Biol. Chem.* **273**, 18528-18537.

Stenkula, K. G., Lizunov, V. A., Cushman, S. W. and Zimmerberg, J. (2010). Insulin controls the spatial distribution of GLUT4 on the cell surface through regulation of its postfusion dispersal. *Cell Metab.* **12**, 250-259.

Stockli, J., Fazakerley, D. J. and James, D. E. (2011). GLUT4 exocytosis. *J. Cell Sci.* **124**, 4147-4159.

Stolar, M. W. (2002). Insulin resistance, diabetes, and the adipocyte. *Am. J. Health Syst. Pharm.* **59**, S3-S8.

Sun, Y., Bilan, P. J., Liu, Z. and Klip, A. (2010). Rab8A and Rab13 are activated by insulin and regulate GLUT4 translocation in muscle cells. *Proc. Natl. Acad. Sci. USA* **107**, 19909-19914.

Sweeney, G., Garg, R. R., Ceddia, R. B., Li, D., Ishiki, M., Somwar, R., Foster, L. J., Neilsen, P. O., Prestwich, G. D., Rudich, A. et al. (2004). Intracellular delivery of phosphatidylinositol (3,4,5)-trisphosphate causes incorporation of glucose transporter 4 into the plasma membrane of muscle and fat cells without increasing glucose uptake. *J. Biol. Chem.* **279**, 32233-32242.

Sylow, L., Kleinert, M., Pehmøller, C., Prats, C., Chiu, T. T., Klip, A., Richter, E. A. and Jensen, T. E. (2014). Akt and Rac1 signaling are jointly required for insulin-stimulated glucose uptake in skeletal muscle and downregulated in insulin resistance. *Cell. Signal.* **26**, 323-331.

Tan, S.-X., Ng, Y., Burchfield, J. G., Ramm, G., Lambright, D. G., Stockli, J. and James, D. E. (2012). The Rab GTPase-activating protein TBC1D4/AS160 contains an atypical phosphotyrosine-binding domain that interacts with plasma membrane phospholipids to facilitate GLUT4 trafficking in adipocytes. *Mol. Cell. Biol.* **32**, 4946-4959.

Taniguchi, C. M., Emanuelli, B. and Kahn, C. R. (2006). Critical nodes in signalling pathways: insights into insulin action. *Nat. Rev. Mol. Cell Biol.* **7**, 85-96.

Tanti, J.-F., Gremeaux, T., Grillo, S., Calleja, V., Klippel, A., Williams, L. T., Van Obberghen, E. and Le Marchand-Brustel, Y. (1996). Overexpression of a constitutively active form of phosphatidylinositol 3-kinase is sufficient to promote Glut 4 translocation in adipocytes. *J. Biol. Chem.* **271**, 25227-25232.

Tengholm, A. and Meyer, T. (2002). A PI3-kinase signaling code for insulin-triggered insertion of glucose transporters into the plasma membrane. *Curr. Biol.* **12**, 1871-1876.

Toettcher, J. E., Voigt, C. A., Weiner, O. D. and Lim, W. A. (2011). The promise of optogenetics in cell biology: interrogating molecular circuits in space and time. *Nat. Methods* **8**, 35-38.

Tsuchiya, A., Kanno, T., Shimizu, T., Tanaka, A. and Nishizaki, T. (2015). Rac1 and ROCK are implicated in the cell surface delivery of GLUT4 under the control of the insulin signal mimetic diDCP-LA-PE. *J. Pharmacol. Sci.* **128**, 179-184.

Ueda, S., Kitazawa, S., Ishida, K., Nishikawa, Y., Matsui, M., Matsumoto, H., Aoki, T., Nozaki, S., Takeda, T., Tamori, Y. et al. (2010). Crucial role of the small GTPase Rac1 in insulin-stimulated translocation of glucose transporter 4 to the mouse skeletal muscle sarcolemma. *FASEB J.* **24**, 2254-2261.

Virkamäki, A., Ueki, K. and Kahn, C. R. (1999). Protein–protein interaction in insulin signaling and the molecular mechanisms of insulin resistance. *J. Clin. Invest.* **103**, 931-943.

Xu, Y.-K., Xu, K.-D., Li, J.-Y., Feng, L.-Q., Lang, D. and Zheng, X.-X. (2007). Bi-directional transport of GLUT4 vesicles near the plasma membrane of primary rat adipocytes. *Biochem. Biophys. Res. Commun.* **359**, 121-128.

Xu, Y., Melia, T. J. and Toomre, D. K. (2011a). Using light to see and control membrane traffic. *Curr. Opin. Chem. Biol.* **15**, 822-830.

Xu, Y., Rubin, B. R., Orme, C. M., Karpikov, A., Yu, C., Bogan, J. S. and Toomre, D. K. (2011b). Dual-mode of insulin action controls GLUT4 vesicle exocytosis. *J. Cell Biol.* **193**, 643-653.

Yu, C., Cresswell, J., Loffler, M. G. and Bogan, J. S. (2007). The glucose transporter 4-regulating protein TUG is essential for highly insulin-responsive glucose uptake in 3T3-L1 adipocytes. *J. Biol. Chem.* **282**, 7710-7722.